1   **Emergence of antibiotic-specific *Mycobacterium tuberculosis***

2   **phenotypes during prolonged treatment of mice**

3   Elizabeth A Wynn,[a,b,c] Christian Dide-Agossou,[a,c,d] Reem Al Mubarak,[a,c,d] Karen Rossmassler,[a,c,d,e]
4   Victoria Ektnitphong,[f] Allison A Bauman,[f] Lisa M Massoudi,[f] Martin I Voskuil,[c,g] Gregory T
5   Robertson,[c,f] Camille M Moore,[b,c,h†] Nicholas D Walter[a,c,d†#]
6
7   a.   Rocky Mountain Regional VA Medical Center, Aurora, CO, USA
8   b.   Center for Genes, Environment and Health, National Jewish Health, Denver, CO, USA
9   c.   Consortium for Applied Microbial Metrics, Aurora, CO, USA
10   d.   Division of Pulmonary Sciences and Critical Care Medicine, University of Colorado Anschutz Medical
11   Campus, Aurora, CO, USA
12   e.   Linda Crnic Institute for Down syndrome, University of Colorado Anschutz Medical Campus, Aurora, CO,
13   USA
14   f.   Mycobacteria Research Laboratories, Department of Microbiology, Immunology, and Pathology, Colorado
15   State University, Fort Collins, CO, USA
16   g.   Department of Immunology and Microbiology, University of Colorado Anschutz Medical Campus, Aurora,
17   Colorado, USA
18   h.   Department of Biostatistics and Informatics, University of Colorado Anschutz Medical Campus, Aurora, CO,
19   USA
20

21   Running Head: Antibiotic-specific *M. tuberculosis* phenotypes in mice

22   Abstract: 233 words
23   Text: 4,402 words
24
25   † Nicholas D Walter and Camille M Moore contributed equally to this work.
26   # Corresponding author: Nicholas D Walter, nicholas.walter@cuanschutz.edu
27
28

29

30

ABSTRACT

A major challenge in tuberculosis (TB) therapeutics is that antibiotic exposure leads to changes in the physiologic state of *M. tuberculosis* (*Mtb*) which may enable the pathogen to withstand treatment. While antibiotic-treated *Mtb* have been evaluated in short-term *in vitro* experiments, it is unclear if and how long-term *in vivo* treatment with diverse antibiotics with varying treatment-shortening activity (sterilizing activity) affect *Mtb* physiologic states differently. Here, we used SEARCH-TB, a pathogen-targeted RNA-sequencing platform, to characterize the *Mtb* transcriptome in the BALB/c high-dose aerosol infection mouse model following 4-week treatment with three sterilizing and three non-sterilizing antibiotics. Certain transcriptional changes were concordant among most antibiotics, including decreased expression of genes associated with protein synthesis and metabolism, and the induction of certain genes associated with stress responses. However, the magnitude of this concordant response differed between antibiotics. Sterilizing antibiotics rifampin, pyrazinamide, and bedaquiline generated a more quiescent *Mtb* state than did non-sterilizing antibiotics isoniazid, ethambutol, and streptomycin, as indicated by decreased expression of genes associated with translation, transcription, secretion of immunogenic proteins, metabolism, and cell wall synthesis. Additionally, we identified distinguishing transcriptional effects specific to each antibiotic, indicating that different mechanisms of action induce distinct patterns of cellular injury. In addition to elucidating *Mtb* physiologic changes associated with antibiotic stress, this study demonstrates the value of SEARCH-TB as a highly granular pharmacodynamic assay that reveals antibiotic effects that are not apparent based on culture alone.

INTRODUCTION

Tuberculosis (TB) is the leading cause of death from infection globally, killing approximately 1.2 million people each year.[1] Because standard antibiotic treatment regimens require 4 to 6 months to reliably cure drug-susceptible TB,[2] there is an urgent need for new antibiotic combinations capable of curing all forms of TB more quickly.[3]

One reason that months-long treatment is required to reliably cure TB is that antibiotic exposure changes the physiologic state of *M. tuberculosis* (*Mtb*).[4] The physiologic state of *Mtb* is a key determinant of antibiotic activity.[5–8] However, there is a paucity of information about the physiologic processes of *Mtb* in an *in vivo* setting or how they might differ depending on an antibiotic's mechanism of action. Attention has historically focused on the direct mechanism of action of antibiotics (*i.e.,* the molecular interaction of an antibiotic with its target protein). However, for *Mtb* that are not immediately killed by initial antibiotic exposure, the immediate injury caused by antibiotic-target binding initiates a cascade of secondary, indirect physiologic perturbations,[9] resulting in chronically stressed bacteria. *Mtb* that survive long-term treatment, and therefore have the potential to cause relapse, are likely shaped by the specific nature of the injury (*i.e.,* the mechanism of action of a given antibiotic). The effect of antibiotics on *Mtb* physiologic processes has been studied extensively in short-term *in vitro* experiments,[10–15] but short-term exposure in axenic culture may not replicate the physicochemical conditions and dynamic pharmacokinetics encountered during chronic *in vivo* exposure. Here, the use of a novel targeted RNA-seq platform called SEARCH-TB[16] enabled us to characterize *Mtb* that emerge during prolonged treatment with diverse antibiotics in mice.

74   While all antibiotics included in conventional combination regimens are thought to

75   contribute to cure to some degree, certain antibiotics play a more pronounced role in shortening

76   the time required to cure TB.[17] Historically, antibiotics such as rifampin, pyrazinamide, and

77   bedaquiline, which have potent treatment-shortening activity, have been described as

78   "sterilizing" while antibiotics such as isoniazid, streptomycin, and ethambutol, which may have

79   bactericidal activity but contribute only modestly to shortening the time needed to achieve a non-

80   relapsing cure, have been described as "non-sterilizing."[18]

81   In this study, we compared the long-term effect of three canonical sterilizing antibiotics

82   (rifampin, bedaquiline, pyrazinamide) and three canonical non-sterilizing antibiotics (isoniazid,

83   streptomycin, ethambutol) over a 28-day treatment period in the BALB/c high-dose aerosol

84   infection mouse model. We first identified *Mtb* transcriptional changes that were common to

85   most of the antibiotics assessed, then compared the effect of sterilizing versus non-sterilizing

86   antibiotics, and finally characterized transcriptional features unique to each antibiotic.

87   **METHODS**

88   **1. Murine experiments and RNA extraction**

89   Experiments used the BALB/c high-dose aerosol infection model, which is central to

90   contemporary TB drug development.[19] Female BALB/c mice, 6 to 8 weeks old, were exposed to

91   aerosol (Glas-Col) with *Mtb* Erdman strain, resulting in 4.55 ± 0.03 (SEM) $\log_{10}$ colony forming

92   units (CFU) in lungs on day one. Mice euthanized after 11 and 19 days (when clinical

93   deterioration required euthanasia) served as pre-treatment and untreated control groups. Starting

94   day 11, mice were treated via oral gavage five days a week for 28 days before euthanasia. We

95   used established human-equivalent doses of all antibiotics (Table S1) except for bedaquiline

96   which was administered at one-fifth of the human-equivalent dose because the full human-

97   equivalent dose resulted in *Mtb* burden too low for reliable SEARCH-TB profiling. Lungs were

98   flash frozen before CFU enumeration and RNA extraction as recently described.[16] All animal

99   procedures were supervised by the Colorado State University Animal Care and Use Committee

100   and conducted according to established guidelines.

101   **2. RNA sequencing, and data preparation**

102   Sequence analysis of samples was performed via SEARCH-TB following recently

103   described methods.[16] Briefly, RNA was reverse transcribed, and cDNA targets were then

104   amplified using the SEARCH-TB panel. Libraries were sequenced on an Illumina NovaSeq6000.

105   We followed the bioinformatic analysis and quality control pipeline as recently described.[16]

106   **3. Statistical Analysis**

107   Following normalization with DESeq2's variance stabilizing transformation (VST),[20] we

108   performed principal component analysis (PCA) on the 500 most variable genes. We estimated

109   differential expression by fitting negative binomial generalized linear models to each gene using

110   edgeR.[21] Likelihood ratio tests were used to compare gene expression between groups.

111   To identify groups of genes with similar expression patterns across conditions, we

112   performed hierarchical clustering of the predicted expression values obtained from the edgeR

113   models after filtering out invariant genes (*i.e.,* not differentially expressed between any two

114   conditions). Then, using Euclidean distance with Ward's method,[22] we clustered the genes based

115   on the predicted expression values for each condition. To further visualize the expression

116   patterns for individual clusters, we used sample-specific, scaled VST normalized expression

117   values averaged across the genes in each cluster (Figure S1). Using analysis of variance

118   (ANOVA) and post-hoc pairwise t-tests, we evaluated between-group differences for each

119   cluster using these scaled expression values.

120   We performed functional enrichment analysis using gene categories established by Cole

121   et al.[23] and curated from the literature (Table S2) using the hypergeometric test in the hypeR

122   package[24] to evaluate whether genes differentially expressed in pairwise comparisons between

123   conditions were overrepresented in each gene set. Enrichment analysis was run twice, using

124   significantly upregulated and significantly downregulated genes separately. Gene categories with

125   fewer than 8 genes were excluded. All analyses were performed using R (v4.3.1) and

126   comparisons were considered statistically significant when Benjamini-Hochberg adjusted *p*-

127   values[25] were less than 0.05. Gene expression for individual gene categories was visualized using

128   sample-specific scaled VST normalized expression values averaged across the genes in the

129   category (Figure S1). Differential expression, functional enrichment, and visualizations can be

130   evaluated interactively using an Online Analysis Tool [https://microbialmetrics.org/analysis-

131   tools/].

RESULTS

1. Bactericidal effect of antibiotic treatments

134   We first characterized the antibiotic effect based on changes in colony forming units

135   (CFU), which estimates the number of bacilli capable of growth on solid agar (**Fig. 1a**). In pre-

136   treatment control mice sacrificed on post-infection day 11, the average lung CFU burden was

137   6.78 $\log_{10}$. In untreated control mice, which were maintained without treatment until post-

138   infection day 19 when clinical deterioration required euthanasia, the average lung CFU burden

139   was 7.91 $\log_{10}$. The average increase of 0.14 $\log_{10}$ per day between days 11 and 19 indicated

140   rapid bacterial replication. Pyrazinamide and ethambutol had a static effect, preventing an

141   increase in CFU burden relative to the pre-treatment control but not reducing the CFU burden

142   after 28 days of treatment. Streptomycin reduced lung CFU by 0.5 $\log_{10}$ relative to the pre-

143   treatment control. Rifampin and isoniazid had bactericidal activity, reducing CFU by 1.05 and

144   1.06 $\log_{10}$ relative to pre-treatment control, respectively. Bedaquiline had the greatest

145   bactericidal effect, reducing CFU by 2.64 $\log_{10}$.

146   **2.   Clustering of antibiotic-induced transcriptional change**

147   Principal Component Analysis of the SEARCH-TB results showed that samples from each

148   antibiotic clustered distinctly from one another (**Fig. 1b**), demonstrating that antibiotics with

149   unique mechanisms of action affect *Mtb* differently. The untreated control (19 days after aerosol

150   infection) was distinct from the pre-treatment control (11 days after aerosol infection), consistent

151   with the effect of adaptive immunity, which is known to occur around day 14.[26] To isolate the

152   effect of antibiotics rather than immunity, we selected the untreated control as our primary

153   reference. The number of *Mtb* genes significantly altered by antibiotic exposure ranged from 430

154   (ethambutol) to 1,545 (bedaquiline) (**Fig. 1c-h**), indicating that each antibiotic stress induced

155   broad changes in bacterial physiological state. To visualize the differences between antibiotics,

156   we performed unsupervised hierarchical clustering based on the average expression of

157   differentially expressed genes (**Fig. 1i**). Of the antibiotics evaluated, ethambutol was the most

158   similar to the untreated control. Isoniazid, streptomycin, pyrazinamide, and rifampin clustered

159   together and were distinct from the transcriptional changes caused by bedaquiline.

160   Unsupervised clustering of differentially expressed genes revealed that certain clusters of

161   genes behaved concordantly among most antibiotics, while others behaved discordantly. For all

162   antibiotics except ethambutol, genes in Cluster 1 (N=639) exhibited increased expression relative

163   to untreated control (**Fig. 1i**). The magnitude of induction of Cluster 1 genes varied between

164   antibiotics (**Fig. 1j**), with greater increase for bedaquiline than for any other antibiotic (*p*-value

165   relative to the closest antibiotic= 0.0003). Conversely, for all antibiotics except ethambutol,

166   genes in Cluster 4 (N=731) had decreased expression relative to the untreated control (**Fig. 1i**),

167   with greater decreases for bedaquiline and rifampin than for isoniazid, streptomycin, and

168   pyrazinamide (**Fig. 1k**). The remaining clusters (2, 3, 5, and 6) identified genes affected in

169   distinct ways by antibiotics with different mechanisms of action (average expression plots in

170   Supplemental Fig. S2), consistent with the emergence of antibiotic-specific injury responses that

171   are discussed further below. Functional enrichment for each cluster is summarized in

172   Supplemental File 1.

173   **3. Concordant *Mtb* transcriptional responses to diverse antibiotic exposures**

174   This section describes the transcriptional responses that were shared among most

175   antibiotic exposures. As described above, ethambutol did not change CFU, clustered with the

176   untreated control and had the smallest number of differentially expressed genes relative to

177   untreated control (**Fig 1h**). To characterize effective antibiotic treatment, ethambutol was

178   therefore excluded from our description of concordant transcriptional responses below. For

179   individual mice, we summarized the average normalized expression of genes in established

180   biological categories (Supplemental Table S2) (**Fig. 2**). For each of the Figure 2 plots,

181   Supplemental Figure S3 includes a corresponding heatmap that summarizes the average

182   expression of individual genes in each category. Statistical results of the functional enrichment

183   analysis are provided in Supplemental File 2.

184   *Suppressed expression of genes associated with protein translation*

185   Antibiotics concordantly decreased the expression of the primary ribosomal protein genes

186   relative to the untreated control, consistent with slowing of protein synthesis (**Fig. 2a**). By

187   contrast, the four "alternative" ribosomal protein genes involved in stress-induced ribosomal

188   remodeling[27,28] had sustained or increased expression (**Fig. 2b**) (gene set too small for statistical

189   functional enrichment evaluation). Antibiotics decreased expression of the protein translation

190   and modification category that includes genes responsible for translational initiation, promotion

191   of tRNA binding, elongation, termination, and protein folding (**Fig. 2c**) (statistically significant

192   in functional enrichment analysis for pyrazinamide, rifampin, and bedaquiline).

193   *Decreased expression of immunogenic secretory proteins*

194   Relative to untreated control, antibiotics decreased expression of the ESX-1 secretion

195   system, including *esxA* and *esxB,* which encode the highly-immunogenic early secretory

196   antigenic 6 kDa (ESAT-6) and culture filtrate protein 10 (CFP-10), respectively (**Fig. 2d**)

197   (statistically significant in functional enrichment analysis for all except ethambutol and

198   streptomycin). Antibiotics decreased expression of the ESX-3 system that secretes peptides that

199   activate neutrophil and macrophages (**Fig. 2e**). Finally, antibiotics appeared to decrease

200   expression of the three genes coding for the Antigen 85 complex (**Fig. 2f**), a secreted protein

201   essential for survival within macrophages which also helps to maintain the *Mtb* cell wall integrity

202   by catalyzing the transfer of mycolic acids to cell wall (gene set too small for statistical

203   functional enrichment analysis).[29]

204   *Metabolic slowing and adaptation*

205   Relative to the untreated control, antibiotics significantly suppressed expression of genes

206   coding for ATP synthetases (**Fig. 2g**). Oxidative phosphorylation appeared to transition from the

207   primary cytochrome *bcc/aa3* supercomplex (downregulated) to the less-efficient cytochrome *bd*

208   oxidase (upregulated), which has been implicated in persistence under environmental and

209   antibiotic stress[30] (**Fig. 2h-i**) (gene sets too small for statistical functional enrichment

210   evaluation). Antibiotics were associated with decreased expression of TCA cycle genes (**Fig. 2j**)

211   (all except ethambutol and rifampin were statistically significant in functional enrichment

212   analysis). Respiratory slowing was not accompanied by the expected increased expression of

213   glyoxylate bypass genes, an alternative pathway previously implicated in antibiotic tolerance.[31]

214   Genes associated with carbon storage such as triacylglycerol were also not upregulated.

215   Specifically, *tgs1,* a gene in the DosR regulon which codes for triacylglycerol synthase

216   previously associated with lipid accumulation during treatment,[32] had significantly decreased

217   expression after exposure to all drugs except ethambutol and isoniazid (see Online Analysis

218   Tool).

219   *Decreased synthesis of mycolic acids and PDIM*

220   Antibiotics significantly reduced the expression of Rv2524c (*fas*), the gene coding for

221   fatty acid synthetase I, indicating a slowdown in the first step of mycolic acid synthesis (see

222   Online Analysis Tool). All antibiotics except ethambutol appeared to decrease expression of

223 Phthiocerol dimycocerosate (PDIM), suggesting potential decreased virulence of the antibiotic-

224 stressed phenotypes[33] (**Fig. 2k**) (statistically significant in functional enrichment analysis for all

225 antibiotics except ethambutol and rifampin).

226 *Regulation of growth: sigma factors*

227   Consistent with transition to a quiescent phenotype, antibiotics resulted in significantly

228 lower expression of *sigA*, which codes for the primary 'housekeeping' sigma factor necessary for

229 growth, relative to untreated control (see Online Analysis Tool). Other sigma factors were

230 affected differently by individual antibiotics and are discussed in Section 5 below.

231 *Modulation of stress responses*

232   Antibiotics induced expression of genes for toxins that act post-transcriptionally to

233 reprogram *Mtb* in response to stress (**Fig. 2l**) (statistically significant in functional enrichment

234 analysis for streptomycin, pyrazinamide, and bedaquiline). However, as described below, the

235 pattern of which toxin genes had increased expression differed depending on antibiotic exposure.

236 Consistent with the change previously observed with the standard 4-drug regimen,[16] mammalian

237 cell entry (*mce*) operons, initially identified as *Mtb* virulence adaptations and more recently

238 implicated in stress adaptation,[34] appeared to have increased expression of Mce-2 and Mce-3

239 operons with all drugs except ethambutol (**Fig. 2m-n**) (gene sets too small for statistical

240 functional enrichment evaluation).

241 **4. Transcriptional response to sterilizing versus non-sterilizing antibiotics**

242   Comparison of canonical sterilizing antibiotics (rifampin, pyrazinamide, bedaquiline)

243   with non-sterilizing antibiotics (isoniazid, streptomycin, ethambutol) suggests that sterilizing

244   drugs generate a more quiescent *Mtb* phenotype, as indicated by genes associated with

245   translation, transcription, secretion of immunogenic proteins, metabolism, and cell wall

246   synthesis. Specifically, expression of genes coding for primary ribosomal proteins, a basic metric

247   of bacterial activity, was suppressed to a significantly greater degree by bedaquiline than by any

248   non-sterilizing antibiotic (**Fig. 2a**). Rifampin and pyrazinamide suppressed primary ribosomal

249   protein gene expression significantly more than two (isoniazid, ethambutol) of three non-

250   sterilizing antibiotics. As discussed above, expression of the protein translation and modification

251   gene category was decreased significantly for the sterilizing antibiotics but not for the non-

252   sterilizing antibiotics. Expression of the gene for RNA polymerase subunit A (*rpoA*) was

253   significantly decreased by all sterilizing antibiotics but not by any non-sterilizing antibiotics.

254   Similarly, RNA polymerase subunit Z (*rpoZ)* was significantly decreased by all sterilizing

255   antibiotics and only one (isoniazid) of the non-sterilizing antibiotics. All three sterilizing

256   antibiotics had significantly decreased expression of *esxA,* the gene coding for ESAT-6, relative

257   to isoniazid and ethambutol. Expression of the gene coding for isocitrate lyase (*icl1*), the first

258   step of the glyoxylate bypass, was decreased significantly by all three sterilizing antibiotics but

259   by none of the non-sterilizing antibiotics.

260   Expression of DosR regulon genes, which respond to hypoxia, carbon monoxide and

261   nitric oxide encountered within host immune effector cells, was significantly reduced by all

262   sterilizing drugs but not by the non-sterilizing drugs (**Fig. 3a**). Because bacterial DosR

263   expression has previously been linked to the intensity of immune activation,[16,35] we plotted the

264   average scaled expression values for the ESX-1, ESX-3, and Antigen 85 genes against mean

265   normalized expression of DosR regulon genes (**Fig. 3b-d**). Expression of ESX-1, ESX-3, and

266   Antigen 85 were correlated with expression of the DosR regulon (R^2=0.7, R^2=0.745, R^2=0.5,

267   respectively), suggesting a link between bacterial phenotype and immune activation.

268   **5. Distinguishing effects of individual antibiotics**

269   Finally, we considered differences in transcriptional changes induced by each individual

270   antibiotic exposure. Despite the existence of shared transcriptional changes discussed above,

271   direct pairwise comparison between antibiotic exposures revealed that each antibiotic resulted in

272   a distinct *Mtb* transcriptional response (**Fig. 4a**). Supplemental file 3 summarizes the categorical

273   enrichment of each antibiotic to one another. Key observations from these tables are highlighted

274   below.

275   ***Bedaquiline.*** Although evaluated at one-fifth the human-equivalent dose, bedaquiline induced

276   the greatest transcriptional change of any antibiotic, significantly altering expression of 1,545

277   genes relative to untreated control (**Fig. 1c**). The bedaquiline-treated phenotype was distinct,

278   with at least 662 genes differentially expressed relative to any other antibiotic (bottom row of

279   **Fig. 4a**). Inhibition of ATP synthetase via 4-week bedaquiline treatment led to a profoundly

280   quiescent, inactive *Mtb* population, consistent with an energy-restricted phenotype. Specifically,

281   relative to all antibiotics other than pyrazinamide, bedaquiline significantly decreased the

282   expression of genes coding for primary ribosomal proteins and genes associated with the

283   synthesis and modification of macromolecules. Bedaquiline suppressed the ESX1 locus to a

284   significantly greater degree than isoniazid, streptomycin, or ethambutol. Additionally,

285   bedaquiline induced greater expression of certain stress responses. Specifically, relative to any

286   antibiotic other than streptomycin, bedaquiline induced significantly greater expression of genes

287   for stressed-induced toxin/antitoxin modules. Relative to any other antibiotic, bedaquiline

288   induced greater expression of sigma factor F, which directs growth arrest in response to diverse

289   stresses (**Fig. 4b**).[36]

290   ***Rifampin.*** Evaluated at the existing standard human-equivalent dose, rifampin had the second-

291   strongest effect on the *Mtb* transcriptome, significantly altering the expression of 1,000 genes

292   relative to untreated control (**Fig. 1d**). The rifampin-treated phenotype was distinct, with at least

293   496 genes differentially expressed relative to any other antibiotic (second from bottom row of

294   **Fig. 4a**). Rifampin resulted in significantly higher expression of genes involved in the cell wall

295   than all antibiotics except ethambutol and significantly higher expression of PDIM than all

296   antibiotics except ethambutol and isoniazid. Rifampin had significantly lower expression of the

297   primary housekeeping sigma factor A than any antibiotic other than pyrazinamide, consistent

298   with the regulation of a quiescent phenotype (**Fig. 4b** and Online Analysis Tool). Rifampin was

299   distinct from all other antibiotics in having significantly increased expression of *sigE,* which

300   codes for sigma factor E that mediates slower growth under stress conditions.[37] All other

301   antibiotics had significantly decreased expression of *sigE.* Rifampin resulted in significantly

302   lower expression of genes coding for chaperones and heat shock proteins and the enduring

303   hypoxic response[38] than any other antibiotic. Rifampin-treated *Mtb* had significantly lower

304   expression of the DosR regulon than *Mtb* treated with any antibiotic except bedaquiline.

305   ***Pyrazinamide.*** Pyrazinamide at human-equivalent dosing for 4 weeks resulted in broad changes

306   in the *Mtb* transcriptome, significantly altering the expression of 822 genes relative to untreated

307   control (**Fig. 1f**). Because pyrazinamide had a static effect on CFU (no change relative to pre-

308   treatment control, **Fig. 1a**), Pyrazinamide appears to induce adaptation of the existing *Mtb*

309   population rather than selection of a pre-existing sub-population. Relative to rifampin,

310   pyrazinamide had significantly higher expression of genes coding for the DosR regulon and the

311   Antigen 85 complex as well as genes involved in beta-oxidation, electron transport, and toxin-

312   antitoxin modules. Pyrazinamide clustered with isoniazid based on global similarity (**Fig. 1b,1i**)

313   and relatively few genes were differentially expressed between pyrazinamide and isoniazid (96

314   significant genes, **Fig. 4a**), yet the pyrazinamide phenotype appeared less active than the

315   isoniazid phenotype, with significantly lower expression of genes involved in protein translation

316   and modification, ribosomal protein synthesis, and synthesis and modification of

317   macromolecules.

318   *Isoniazid.* Isoniazid at human-equivalent dosing significantly altered the expression of 650 genes

319   relative to untreated control (**Fig. 1g**). Inhibition of mycolic acid synthesis by isoniazid was

320   associated with higher expression of mycolic acid synthesis genes of the *kas* operon than any

321   antibiotic other than ethambutol, suggesting continuing *Mtb* compensation to the isoniazid

322   mechanism of action (**Fig. 4c,** Online Analysis Tool). Isoniazid also had significantly higher

323   expression of DosR regulon genes compared to all antibiotics except ethambutol, suggesting

324   adaptation to continued immune-mediated nitric oxide or hypoxic stress.

325   *Streptomycin.* Streptomycin at human-equivalent dosing significantly altered the expression of

326   850 genes relative to untreated control (**Fig 1e**). The streptomycin phenotype was distinct, with

327   at least 245 genes differentially expressed relative to any other antibiotic (**Fig. 4a**). Protein

328   synthesis inhibition by streptomycin resulted in significantly higher expression of toxin-antitoxin

329   pairs and of the enduring hypoxic response compared to any antibiotic other than bedaquiline.

330   Streptomycin also resulted in significantly higher expression of chaperones and heat shock genes

331   compared to any antibiotic other than ethambutol and significantly higher expression of genes

332   associated with the response to oxidative stress than any antibiotic other than ethambutol or

333   bedaquiline.

334   ***Ethambutol.*** Human-equivalent dosing of ethambutol induced the least transcriptional change

335   among the antibiotics assessed, with 430 genes significantly altered relative to untreated control

336   (**Fig. 1h**). The ethambutol transcriptome clustered with the untreated control (**Fig. 1i**), and was

337   distinct from other antibiotics in most of the discrete processes shown in Figure 2.

338   **DISCUSSION**

339   We found that 28-day treatment of mice with six different antibiotics led to emergence of

340   antibiotic-specific *Mtb* transcriptional responses. Antibiotics differed both in the magnitude of

341   transcriptional change they induced in *Mtb* and the specific sets of genes up- or down-regulated.

342   Broadly, rifampin, pyrazinamide, and bedaquiline, the antibiotics with enhanced treatment-

343   shortening activity (historically described as sterilizing), led to a less active bacterial phenotype

344   than did antibiotics with lesser treatment-shortening activity (historically described as non-

345   sterilizing).

346   *Mtb* phenotypes that lack resistance-conferring mutations, yet survive extended drug

347   exposure *in vivo,* are viewed as a central obstacle to shortening the time required to cure TB.[39,40]

348   Our results suggest that different individual drugs result in distinct *in vivo* "persister" *Mtb*

349   phenotypes. Rather, antibiotics with different mechanisms of action represent distinct injuries

350   that condition the physiologic state of *Mtb* in distinct ways. While some broad transcriptional

351   responses are shared among antibiotics (*e.g.,* down-regulation of genes associated with synthesis

352   of macromolecules and metabolism and up-regulation of certain stress responses), each antibiotic

353   also had unique effects on the *Mtb* transcriptome.

354   Of particular interest are sterilizing antibiotics known to play an outsized contribution to

355   the ability of combination regimens to shorten the time required to TB cure. In this study, we

356   selected three antibiotics with enhanced treatment-shortening activity – rifampin, pyrazinamide,

357   and bedaquiline – that are central to contemporary regimen development and are included in

358   recent and ongoing human trials. The SEARCH-TB analysis revealed that rifampin,

359   pyrazinamide, and bedaquiline suppressed bacterial activity to a greater degree than did

360   isoniazid, streptomycin, and ethambutol. This finding aligns with our previous observations

361   using the RS ratio® assay in the same mouse sample set which showed that rifampin,

362   pyrazinamide, and bedaquiline decreased ribosomal RNA synthesis to a greater degree than

363   antibiotics with lesser treatment-shortening activity.[41] Combined with the RS ratio results, the

364   SEARCH-TB data suggest that a common effect of antibiotics with potent treatment-shortening

365   activity is the induction of a more inactive *Mtb* phenotype. Our findings suggest, but cannot

366   definitively resolve, two potential interpretations for the observed association between treatment-

367   shortening activity and decreased bacterial activity. First, a more quiescent phenotype may

368   represent a functional physiologic adaptation that enables *Mtb* to survive exposure to rifampin,

369   pyrazinamide, or bedaquiline, but is less crucial for surviving isoniazid, streptomycin, and

370   ethambutol, streptomycin, and ethambutol. Alternatively, the more quiescent phenotype could be

371   a "vital sign" of bacterial injury, signaling more severe stress and resultant bacterial dysfunction.

372   *Mtb* population experiencing energy starvation (bedaquiline), or transcriptional inhibition

373   (rifampin) may be functionally incapacitated or in a pre-terminal state.

374   For several antibiotics, the DosR regulon, which responds to nitric oxide and hypoxia *in*

375   *vivo,* was downregulated relative to the untreated controls. This is consistent with previous

376   observations in *Mtb* infected humans receiving antibiotic treatment[35] and in mice treated with

377   HRZE.[16] Because antibiotics do not directly target generation of nitric oxide or restrict oxygen,

378   the changes in the expression of the DosR regulon after antibiotic exposure is likely an indirect

379   effect of treatment. Since activation of macrophages and neutrophils results in increased nitric

380   oxide[42,43] the observed downregulation in the DosR regulon after some antibiotic treatments may

381   correspond to decreased inflammation. This theory is corroborated in the correlation of DosR

382   regulon expression and the expression of the ESX-1 and ESX-3 systems, which have been linked

383   with macrophage and neutrophil activation.[44,45] If the observed fluctuation in the DosR regulon

384   across antibiotic treatments is, in fact, a manifestation of host inflammation, this would indicate

385   that antibiotics may impact host-pathogen interactions differently.

386   This work highlights the power of SEARCH-TB as a pharmacodynamic marker. In both

387   preclinical studies and human trials, evaluation of new TB treatment has been hamstrung by

388   limitations of existing culture-based pharmacodynamic markers.[46,47] The fraction of the viable

389   *Mtb* population that is capable of regrowth in culture is uncertain and may vary depending on

390   antibiotic used.[48,49] Additionally, enumeration of bacterial burden provides no information about

391   how antibiotics affect *Mtb* physiologic processes. SEARCH-TB and other indicators of *Mtb*

392   physiologic state such as the RS ratio reveal differences between drugs that appear identical

393   based on burden. For example, we found that CFU did not distinguish between the effects of

394   ethambutol (a weak antibiotic included in the standard regimen to protect against emergence of

395   resistance) and pyrazinamide (an antibiotic shown to have potent treatment-shortening activity

396   when added to combination regimens). By contrast, SEARCH-TB showed that pyrazinamide and

397   ethambutol exposure resulted in profoundly different *Mtb* phenotypes with 1,531 genes or 43%

398   of the transcriptome differentially expressed between the two. Similarly, isoniazid and rifampin,

399   which are conventionally understood to play quite different roles in the existing standard

400   regimen[18], had indistinguishable effects on CFU but resulted in distinct molecular phenotypes.

401   Our results indicate that antibiotics have effects that are not discernable based on the burden of

402   bacilli recovered on solid agar. By evaluating bacterial physiologic processes rather than

403   estimating bacterial burden, SEARCH-TB may reveal hitherto occult antibiotic effects that

404   inform antibiotic development.

405   This report has several limitations. First, this report characterized drug-induced

406   phenotypic change in the lungs of BALB/c mice, which develop loose macrophage aggregates

407   containing intracellular *Mtb*. Other TB mouse models (such as the C3HeB/FeJ mouse) develop

408   necrotic granulomas in which *Mtb* is extracellular and has distinct phenotypic adaptations to

409   local conditions.[50] A high-priority next step is interrogating *Mtb* in diverse models to elucidate

410   the full spectrum of bacterial phenotypes and antibiotic responses. Second, we used the high-

411   dose aerosol infection model because it is a mainstay of contemporary preclinical drug and

412   regimen evaluation.[19] High-dose aerosol infection is lethal if mice are not "rescued" by initiation

413   of antibiotic treatment.[26] In this experiment, untreated mice experienced clinical deterioration

414   requiring humane euthanasia 19 days after aerosol infection. The untreated control therefore

415   could not be temporally matched with the antibiotic-treated mice. Third, all antibiotics were

416   evaluated at a human equivalent dose except bedaquiline which reduced *Mtb* burden below the

417   limits of SEARCH-TB reliability at human equivalent dosing. It is likely that higher or lower

418   drug doses might induce different transcriptional responses. Finally, SEARCH-TB quantifies

419   expression in an entire lesion, inherently representing a population average that does not reveal

420   heterogeneity within the population.

421   Using a novel pathogen-targeted RNA-seq method, we evaluated *Mtb* after 4-weeks of

422   treatment with individual antibiotics *in vivo*, demonstrating that antibiotics with different

423   mechanisms of action lead to distinct *Mtb* phenotypes. Sterilizing antibiotics generated a less

424   active *Mtb* phenotype than non-sterilizing drugs. This report demonstrates the capability of

425   SEARCH-TB to reveal differences in antibiotic effects that are not discernable via conventional

426   microbiologic tools, potentially enabling a new era of pharmacodynamic monitoring in which

427   candidate TB treatments are evaluated *in vivo* based on highly granular assessment of bacterial

428   physiologic processes.

REFERENCES

1. World Health Organization. *Global tuberculosis report 2020*. (2020).

2. Nahid, P. *et al.* Official American Thoracic Society/Centers for Disease Control and Prevention/Infectious Diseases Society of America clinical practice guidelines: Treatment of drug-susceptible tuberculosis. *Clinical Infectious Diseases* **63**, e147–e195 (2016).

3. Dartois, V. A. & Rubin, E. J. Anti-tuberculosis treatment strategies and drug development: Challenges and priorities. *Nature Reviews Microbiology* **20**, 685–701 (2022).

4. Roemhild, R., Bollenbach, T. & Andersson, D. I. The physiology and genetics of bacterial responses to antibiotic combinations. *Nature Reviews Microbiology* **20**, 478–490 (2022).

5. Lenaerts, A., Barry, C. E. & Dartois, V. Heterogeneity in tuberculosis pathology, microenvironments and therapeutic responses. *Immunol. Rev.* **264**, 288–307 (2015).

6. Sarathy, J. P. *et al.* Extreme drug tolerance of mycobacterium tuberculosis in caseum. *Antimicrob. Agents Chemother.* **62**, (2018).

7. Lanni, F. *et al.* Adaptation to the intracellular environment of primary human macrophages influences drug susceptibility of *Mycobacterium tuberculosis*. *Tuberculosis* **139**, 102318 (2023).

8. Abo-Kadoum, M. A., Dai, Y., Asaad, M., Hamdi, I. & Xie, J. Differential Isoniazid Response Pattern between Active and Dormant *Mycobacterium tuberculosis*. *Microb. Drug Resist.* **27**, 768–775 (2021).

9. Koul, A. *et al.* Delayed bactericidal response of *Mycobacterium tuberculosis* to bedaquiline involves remodelling of bacterial metabolism. *Nat. Commun.* **5**, 3369 (2014).

10. Waddell, S. J. *et al.* The use of microarray analysis to determine the gene expression profiles of *Mycobacterium tuberculosis* in response to anti-bacterial compounds. *Tuberculosis* **84**, 263–274 (2004).

11. Boshoff, H. I. M. *et al.* The transcriptional responses of *Mycobacterium tuberculosis* to inhibitors

457   of metabolism: Novel insights into drug mechanisms of action. *J. Biol. Chem.* **279**, 40174–40184

458   (2004).

459   12.   Wilson, M. *et al.* Exploring drug-induced alterations in gene expression in *Mycobacterium*

460   *tuberculosis* by microarray hybridization. *Proc. Natl. Acad. Sci. U. S. A.* **96**, 12833–12838 (1999).

461   13.   Deb, C. *et al.* A novel in vitro multiple-stress dormancy model for *Mycobacterium tuberculosis*

462   generates a lipid-loaded, drug-tolerant, dormant pathogen. *PLoS One* **4**, e6077 (2009).

463   14.   Betts, J. C., Lukey, P. T., Robb, L. C., McAdam, R. A. & Duncan, K. Evaluation of a nutrient

464   starvation model of *Mycobacterium tuberculosis* persistence by gene and protein expression

465   profiling. *Mol. Microbiol.* **43**, 717–731 (2002).

466   15.   Poonawala, H. *et al.* Transcriptomic responses to antibiotic exposure in *Mycobacterium*

467   *tuberculosis*. *Antimicrob. Agents Chemother.* **68**, (2024).

468   16.   Wynn, E. A. *et al.* Transcriptional adaptation of *Mycobacterium tuberculosis* that survives

469   prolonged multi-drug treatment in mice. *MBio* (2023). doi:10.1128/mbio.02363-23

470   17.   Mitchison, D. A. Basic mechanisms of chemotherapy. *Chest* **76**, 771–780 (1979).

471   18.   Mitchison, D. A. Role of individual drugs in the chemotherapy of tuberculosis. *Int. J. Tuberc.*

472   *Lung Dis.* **4**, 796–806 (2000).

473   19.   Gumbo, T., Lenaerts, A. J., Hanna, D., Romero, K. & Nuermberger, E. Nonclinical models for

474   antituberculosis drug development: A landscape analysis. *J. Infect. Dis.* **211**, S83–S95 (2015).

475   20.   Love, M. I., Huber, W. & Anders, S. Moderated estimation of fold change and dispersion for

476   RNA-seq data with DESeq2. *Genome Biol.* **15**, 550 (2014).

477   21.   Robinson, M. D., McCarthy, D. J. & Smyth, G. K. edgeR: A Bioconductor package for differential

478   expression analysis of digital gene expression data. *Bioinformatics* **26**, 139–140 (2010).

479   22.   Murtagh, F. & Legendre, P. Ward's hierarchical agglomerative clustering method: Which

480   algorithms implement Ward's criterion? *J. Classif.* **31**, 274–295 (2014).

481   23. Cole, S. T. *et al.* Erratum: Deciphering the biology of *Mycobacterium tuberculosis* from the

482   complete genome sequence. *Nature* **396**, 190 (1998).

483   24. Federico, A. & Monti, S. HypeR: An R package for geneset enrichment workflows.

484   *Bioinformatics* **36**, 1307–1308 (2020).

485   25. Benjamini, Y. & Hochberg, Y. Controlling the false discovery rate: A practical and powerful

486   approach to multiple testing. *J. R. Stat. Soc. Ser. B* **57**, 289–300 (1995).

487   26. Zhang, N. *et al.* Mechanistic modeling of *Mycobacterium tuberculosis* infection in murine models

488   for drug and vaccine efficacy studies. *Antimicrob. Agents Chemother.* **64**, (2020).

489   27. Prisic, S. *et al.* Zinc regulates a switch between primary and alternative S18 ribosomal proteins in

490   *Mycobacterium tuberculosis*. *Mol. Microbiol.* **97**, 263–280 (2015).

491   28. Kushwaha, A. K. & Bhushan, S. Unique structural features of the *Mycobacterium* ribosome.

492   *Progress in Biophysics and Molecular Biology* **152**, 15–24 (2020).

493   29. Karbalaei Zadeh Babaki, M., Soleimanpour, S. & Rezaee, S. A. Antigen 85 complex as a powerful

494   *Mycobacterium tuberculosis* immunogene: Biology, immune-pathogenicity, applications in

495   diagnosis, and vaccine design. *Microbial Pathogenesis* **112**, 20–29 (2017).

496   30. Mascolo, L. & Bald, D. Cytochrome *bd* in Mycobacterium tuberculosis: A respiratory chain

497   protein involved in the defense against antibacterials. *Progress in Biophysics and Molecular*

498   *Biology* **152**, 55–63 (2020).

499   31. Nandakumar, M., Nathan, C. & Rhee, K. Y. Isocitrate lyase mediates broad antibiotic tolerance in

500   *Mycobacterium tuberculosis*. *Nat. Commun.* **5**, (2014).

501   32. Garton, N. J. *et al.* Cytological and transcript analyses reveal fat and lazy persister-like bacilli in

502   tuberculous sputum. *PLoS Med.* **5**, 0634–0645 (2008).

503   33.   Quigley, J. *et al.* The cell wall lipid PDIM contributes to phagosomal escape and host cell exit of

504   *Mycobacterium tuberculosis*. *MBio* **8**, (2017).

505   34.   Klepp, L. I., Sabio y Garcia, J. & FabianaBigi. Mycobacterial MCE proteins as transporters that

506   control lipid homeostasis of the cell wall. *Tuberculosis* **132**, 102162 (2022).

507   35.   Walter, N. D. *et al.* Transcriptional adaptation of drug-tolerant *Mycobacterium tuberculosis* during

508   treatment of human tuberculosis. *J. Infect. Dis.* **212**, 990–8 (2015).

509   36.   Oh, Y. *et al.* The partner switching system of the SigF sigma factor in *Mycobacterium smegmatis*

510   and induction of the SigF regulon under respiration-inhibitory conditions. *Front. Microbiol.* **11**,

511   588487 (2020).

512   37.   Chauhan, R. *et al.* Reconstruction and topological characterization of the sigma factor regulatory

513   network of *Mycobacterium tuberculosis*. *Nat. Commun.* **7**, (2016).

514   38.   Rustad, T. R., Harrell, M. I., Liao, R. & Sherman, D. R. The enduring hypoxic response of

515   *Mycobacterium tuberculosis*. *PLoS One* **3**, e1502 (2008).

516   39.   Connolly, L. E., Edelstein, P. H. & Ramakrishnan, L. Why is long-term therapy required to cure

517   tuberculosis? *PLoS Med.* **4**, e120 (2007).

518   40.   Mandal, S., Njikan, S., Kumar, A., Early, J. V & Parish, T. The relevance of persisters in

519   tuberculosis drug discovery. *Microbiology (United Kingdom)* **165**, 492–499 (2019).

520   41.   Walter, N. D. *et al. Mycobacterium tuberculosis* precursor rRNA as a measure of treatment-

521   shortening activity of drugs and regimens. *Nat. Commun.* **12**, 1–11 (2021).

522   42.   Braverman, J. & Stanley, S. A. Nitric oxide modulates macrophage responses to *Mycobacterium*

523   *tuberculosis* infection through activation of HIF-1α and Repression of NF-κB. *J. Immunol.* **199**,

524   1805–1816 (2017).

525   43.   Jamaati, H. *et al.* Nitric oxide in the pathogenesis and treatment of tuberculosis. *Frontiers in*

526   *Microbiology* **8**, 281243 (2017).

527   44.   Conrad, W. H. *et al.* Mycobacterial ESX-1 secretion system mediates host cell lysis through

528   bacterium contact-dependent gross membrane disruptions. *Proc. Natl. Acad. Sci. U. S. A.* **114**,

529   1371–1376 (2017).

530   45.   Tufariello, J. A. M. *et al.* Separable roles for *Mycobacterium tuberculosis* ESX-3 effectors in iron

531   acquisition and virulence. *Proc. Natl. Acad. Sci. U. S. A.* **113**, E348–E357 (2016).

532   46.   Dooley, K. E., Phillips, P. P. J., Nahid, P. & Hoelscher, M. Challenges in the clinical assessment

533   of novel tuberculosis drugs. *Advanced Drug Delivery Reviews* **102**, 116–122 (2016).

534   47.   Lenaerts, A. J., DeGroote, M. A. & Orme, I. M. Preclinical testing of new drugs for tuberculosis:

535   Current challenges. *Trends Microbiol.* **16**, 48–54 (2008).

536   48.   Mukamolova, G. V., Turapov, O., Malkin, J., Woltmann, G. & Barer, M. R. Resuscitation-

537   promoting factors reveal an occult population of tubercle bacilli in sputum. *Am. J. Respir. Crit.*

538   *Care Med.* **181**, 174–180 (2010).

539   49.   Chengalroyen, M. D. *et al.* Detection and quantification of differentially culturable tubercle

540   bacteria in sputum from patients with tuberculosis. *Am. J. Respir. Crit. Care Med.* **194**, 1532–1540

541   (2016).

542   50.   Walter, N. D. *et al.* Lung microenvironments harbor *Mycobacterium tuberculosis* phenotypes with

543   distinct treatment responses. *Antimicrob. Agents Chemother.* **67**, (2023).

544   **Figures**
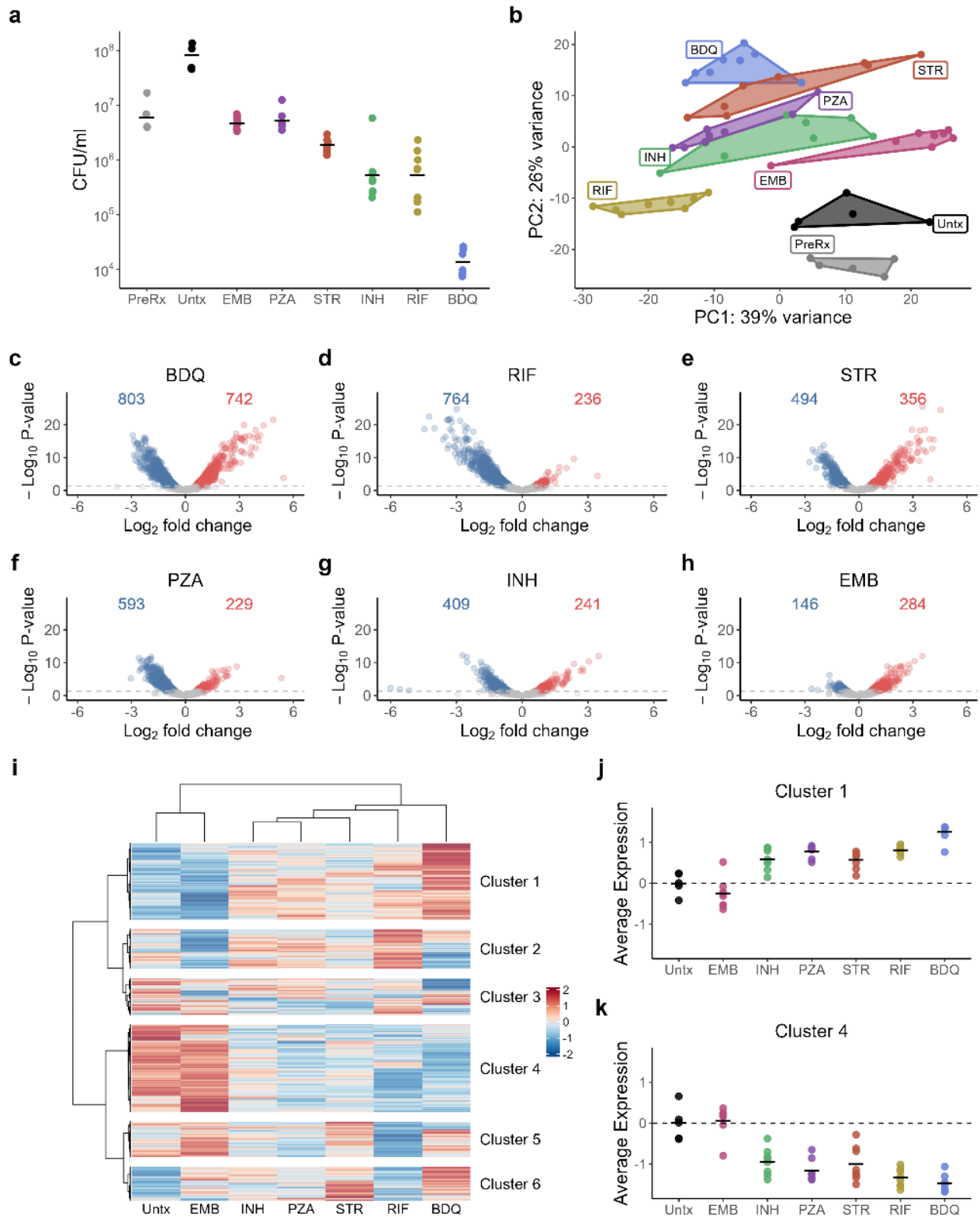
545   **Figure 1**. **a**. *Mtb* CFU burden in the lungs of BALB/c mice after 4-week treatment with individual antibiotics.

546   Circles indicate CFU values from individual mice. Horizontal bars indicate group means. PreRx and Untx indicate

547   control mice sacrificed on the day treatment was initiated or 8 days thereafter, respectively. **b**. Principal Components

548   Analysis (PCA) plot of VST-normalized gene expression data, for the top 500 most variable genes. The first two

549   principal components are shown on the x- and y- axes and each point represents an individual sample. A convex hull

550   highlights antibiotic treatments. **c-h**. Volcano plots summarizing the differential expression between *Mtb* in

551   untreated mice and *Mtb* in (c) BDQ, (d) RIF, (e) STR, (f) PZA, (g) INH, and (h) EMB. The number of genes

552   significantly down- (blue) or upregulated (red) for each antibiotic treatment relative to untreated (adj *p*-value< 0.05)

553   are shown. **i.** Heatmap of gene expression including all genes significantly differentially expressed between at least

554   two treatment conditions (N=2,589). Values are row-scaled, with red and blue indicating higher and lower

555   expression, respectively. Hierarchical clustering of genes identified six broad patterns. **j-k**. Average of VST-

556   normalized, scaled expression across treatments for clusters (j) one and (k) four. Each point represents an individual

557   mouse. Horizontal lines indicate average values. Values are centered around the average value for the untreated

558   samples so that points above and below zero represent upregulation or downregulation relative to untreated,

559   respectively. Abbreviations: Untreated (Untx), Ethambutol (EMB), Isoniazid (INH), Pyrazinamide (PZA),

560   Streptomycin (STR), Rifampin (RIF), Bedaquiline (BDQ).

561
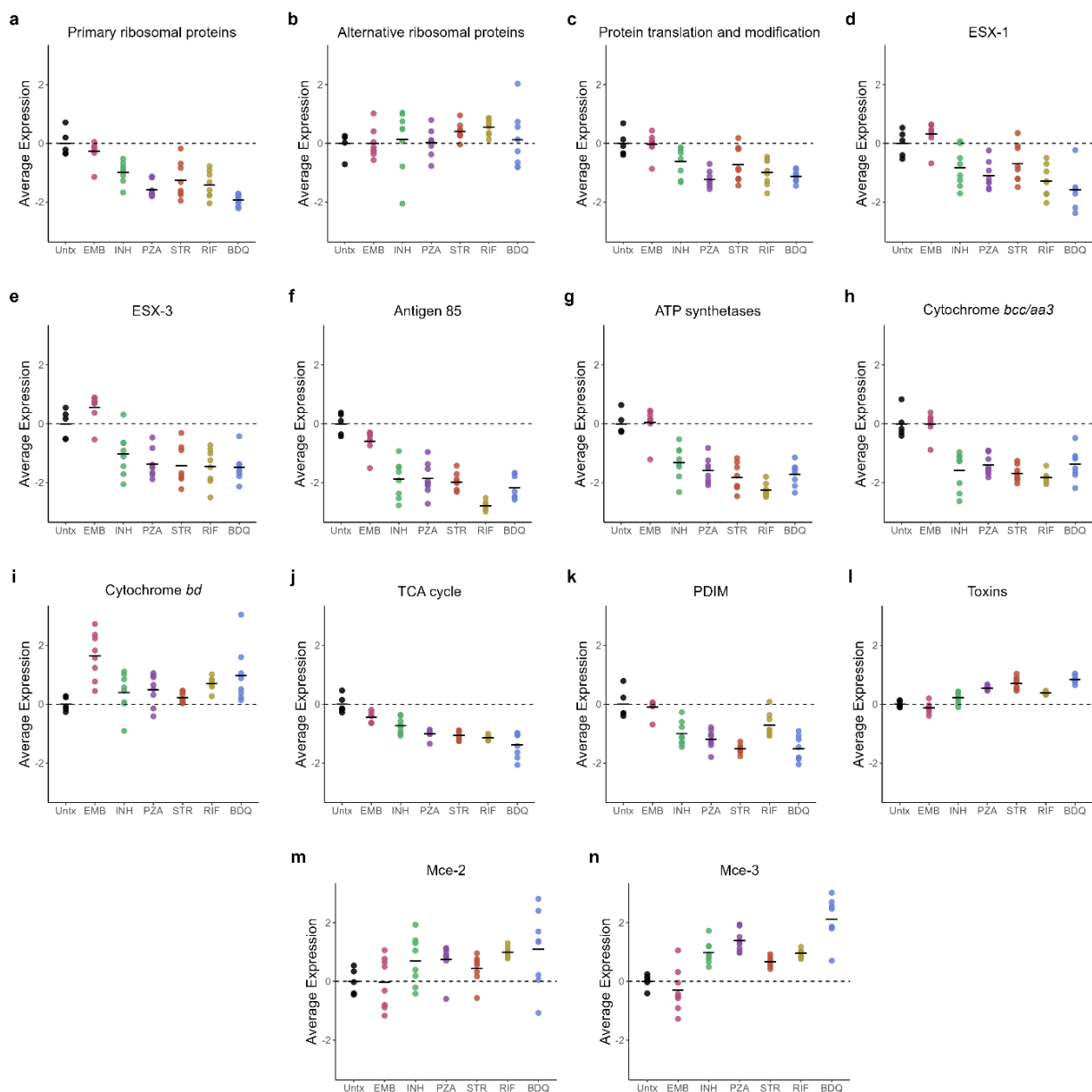
Figure 2. Average of VST-normalized, scaled gene expression across *Mtb* treatments in BALB/c mice for genes in key *Mtb* biological processes: (**a**) primary ribosomal proteins, (**b**) alternative ribosomal proteins, (**c**) protein translation and modification, (**d**) ESX-1, (**e**) ESX-3, (**f**) antigen 85, (**g**) ATP synthesis, (**h**) cytochrome *bcc/aa3*, (**i**) cytochrome *bd*, (**j**) TCA cycle (**k**) PDIM, (**l**) toxins, (**m**) MCE-1, and (**n**) MCE-3. Each point represents an individual mouse. Horizontal lines indicate average values. Values are centered around the average value for the untreated samples so that points above and below zero represent upregulation or downregulation relative to untreated, respectively. Abbreviations: Untreated (Untx), Ethambutol (EMB), Isoniazid (INH), Pyrazinamide (PZA), Streptomycin (STR), Rifampin (RIF), Bedaquiline (BDQ)

569
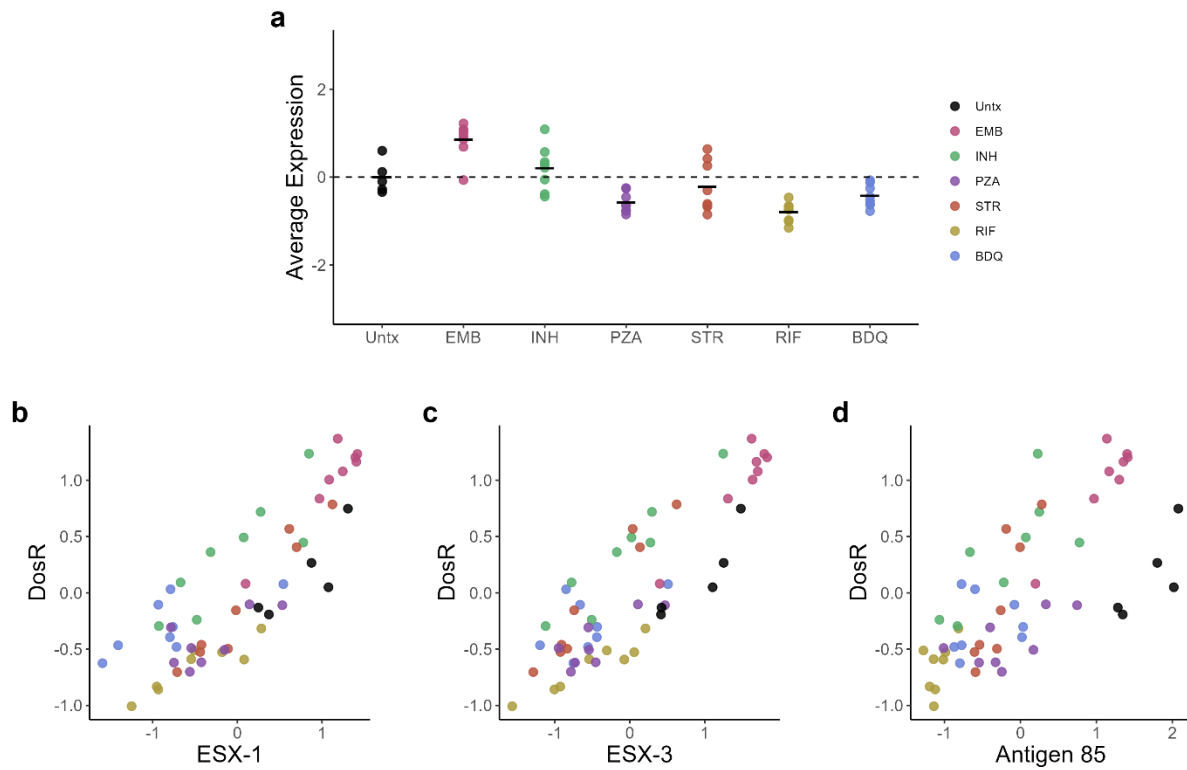
Figure 3 a. Average of VST-normalized, scaled expression across antibiotic treatments for genes in the DosR regulon. **b-c** Correlation between the scaled average expression for categories associated with immune activation and DosR: (**m**) ESX-1, (n) ESX-3, and (o) antigen 85. Each point represents an individual mouse and points are colored by treatment group. Abbreviations: Untreated (Untx), Ethambutol (EMB), Isoniazid (INH), Pyrazinamide (PZA), Streptomycin (STR), Rifampin (RIF), Bedaquiline (BDQ).
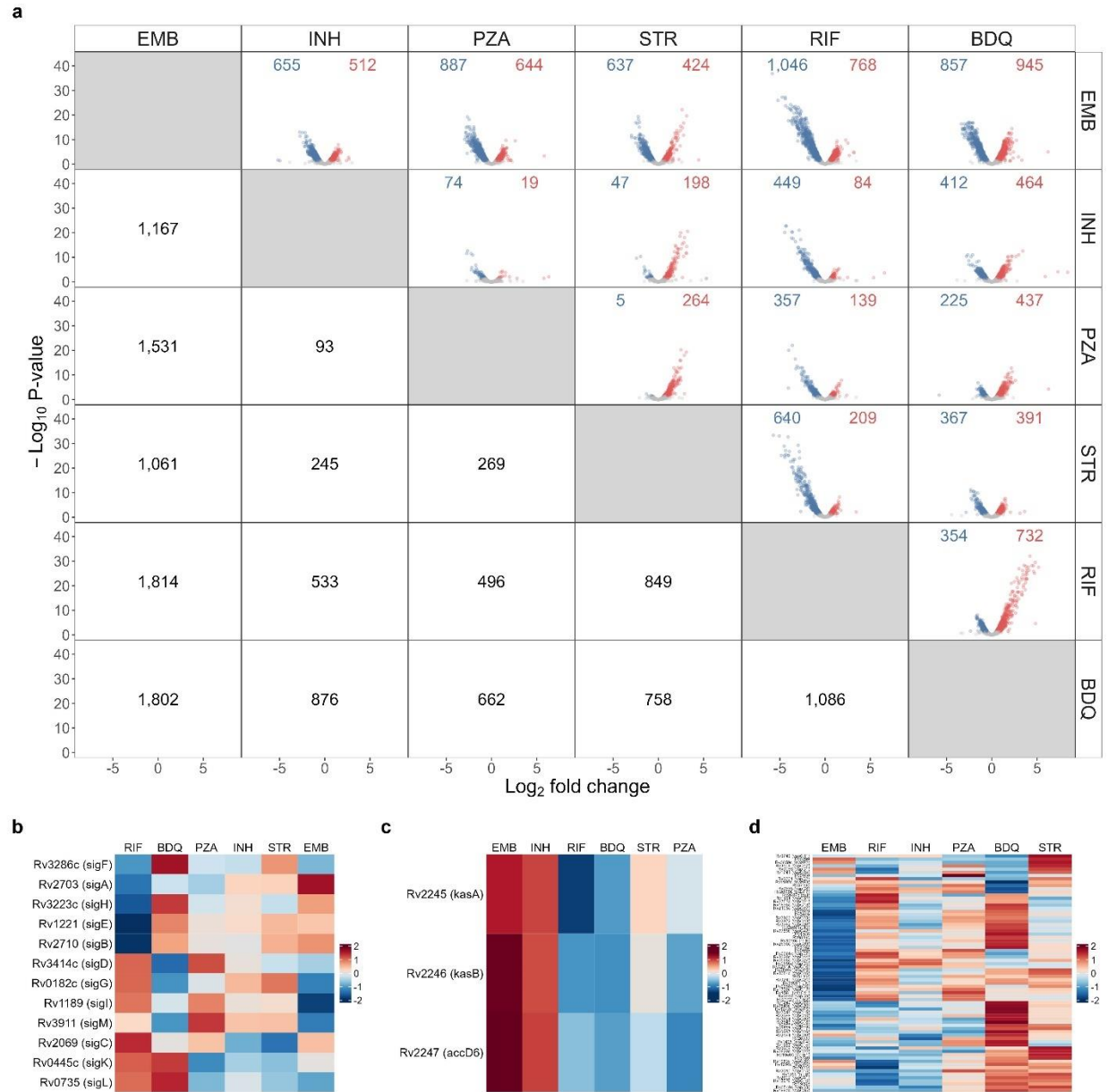
Figure 4 a. Differential expression in pairwise comparison between individual antibiotics. Volcano plots show fold change and significance between the antibiotics labeled in the row and column. The number of genes significantly down- (blue) or upregulated (red) with adj *p*-value< 0.05 in the row versus the column is shown below the diagonal. **b-d** Heatmaps showing the scaled average expression across antibiotic conditions for (**b**) sigma factors, (**c**) the *Kas* operon and (**d**) toxins. Abbreviations: Ethambutol (EMB), Isoniazid (INH), Pyrazinamide (PZA), Streptomycin (STR), Rifampin (RIF), Bedaquiline (BDQ).